

Changing the entrance surface dose and image quality by applying an air mattress to the table commonly used in computed tomography

J.Y. Park¹ and S. Kim²

¹Department of Diagnostic Radiology, Uijeongbu Eulji Medical Center, Eulji University, Gyeonggi-do, Korea

²Department of Radiological Science, Gachon University Medical Campus, Incheon, Korea

► Original article

*Corresponding author:

Sungchul Kim, Ph.D.,

E-mail: ksc@gachon.ac.kr

Received: November 2020

Final revised: August 2021

Accepted: September 2021

Int. J. Radiat. Res., April 2022;
20(2): 425-429

DOI: 10.52547/ijrr.20.2.25

Keywords: Entrance surface dose, air mattress, computed tomography, SNR, CNR.

INTRODUCTION

Various efforts have been made worldwide to minimize the stochastic effects of radiation on patients and operators by minimizing delivered radiation without affecting the efficacy of medical treatments ⁽¹⁾. However, few researchers have attempted to reduce the increase in entrance surface dose (ESD) caused by X-rays scattered by the table. Scattered X-rays have low energy levels, meaning that they are mostly attenuated by the patient's skin, which is a major cause of excessive radiation exposure. Continuous exposure to radiation increases the chances of suffering radiation skin injuries ⁽²⁾. Additionally, it has been reported that diseases induced by radiation, such as necrosis and dermatitis, are difficult to cure ⁽³⁾.

The amount of X-ray scattering depends on the type and thickness of the materials used to construct the table. Currently, acrylic is the most widely used material as it is cheap and simple to process. However, a thickness of at least a 10 mm is required for the table, which results in a high amount of X-ray scattering ⁽⁴⁾. Alternatively, carbon is highly radiolucent and scatters significantly fewer X-rays, which makes it highly suitable as a table material. Unfortunately, carbon's production cost is extremely high ⁽⁵⁾.

ABSTRACT

Background: In this study, the changes in the entrance surface dose (ESD) and image quality were examined when an air mattress was used to reduce the X-ray scattering caused by treatment tables commonly used for computed tomography (CT). **Materials and Methods:** Dual-energy CT (DECT) was used, with the ESD of Alderson Radiation Therapy (ART) phantom measured by scanning with different X-ray tube voltages and X-ray tube currents for three scenarios: when no air mattress was employed, and when a 5 cm or 10 cm thick air mattress was employed. The statistical significance of the changes in ESD and image quality were based on the presence and thickness of the air mattress. Additionally, the variations of the X-ray tube voltage and current for different air mattress thicknesses were investigated using paired *t*-test. **Results:** For all X-ray tube voltages and currents, applying an air mattress significantly improved both the ESD and image quality, with the 5 cm air mattress improving both the ESD and image quality. **Conclusion:** The 5 cm air mattress produced no artifacts in the diagnostic images, and demonstrated a statistically significant reduction in patient ESD during DECT imaging.

In this study, air mattresses of different thicknesses were produced to apply the air gap principle with the aim of minimizing the ESD caused by X-rays scattered by the table during computed tomography (CT) examinations. The optimal air mattress thickness for reducing the ESD without affecting image quality for various tube voltages and currents was also investigated.

MATERIALS AND METHODS

Experimental equipments

Dual-energy CT (DECT) (SOMATOM Definition Flash CT, Siemens Healthcare, Forchheim, Germany) and an Alderson Radiation Therapy (ART) phantom (ARTF-1007, Radiology Support Device, Long Beach, CA, USA) were used in this study. To measure the ESD, optically stimulated luminescent dosimeters (OSLD) NanoDots (Landauer Co., Glenwood, IL, USA), an optically stimulated luminescent (OSL) Microstar Reading System (Landauer Co., Glenwood, IL, USA), and OSL annealing equipment (Serial No. HA-ONH001 (Hanil Nuclear Co., Korea) were used. The air mattresses were developed by connecting $\varnothing 5 \times 200$ cm² and $\varnothing 10 \times 200$ cm² air sticks made with 0.2 mm thick polyurethane (see figure 1, Korean Patent No. 10-1876500, Daesung Life co. Korea).

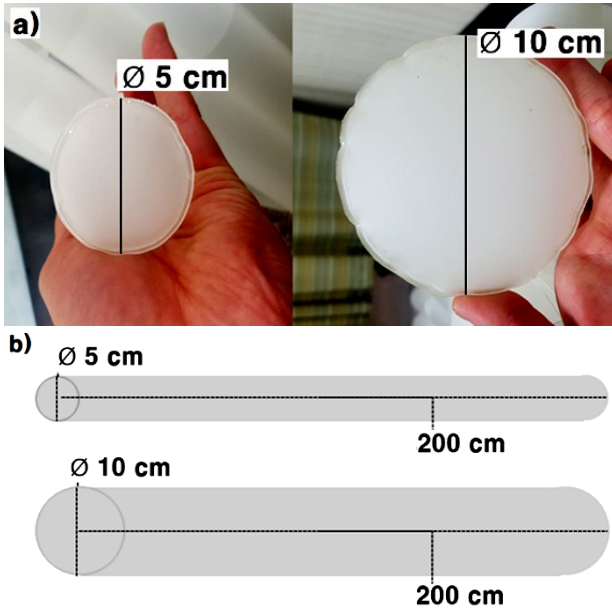


Figure 1. Specification of Air mattress. a) Air stick front View, b) Air Stick side specification.

ESD measurement

Five OSLD NanoDots were attached to the fourth thoracic vertebra (slice 11) of the ART phantom. The 250 mm long scan range was set to include the apex and costophrenic angle (CPA) of the lungs, and the ESD was averaged over five measurements for each variation of the tube voltage and current (table 1). The method was applied for no air mattress, the 5 cm mattress, and the 10 cm mattresses. The images were saved in the standard Digital Imaging and Communications in Medicine (DICOM) format. All OSLD NanoDots were annealed for 60 min prior to the experiments, and the background radiation was measured. The background readings were subsequently subtracted from the measured value to obtain the actual value.

Table 1. ART Phantom CT scan parameters.

Parameter	Topo	Helical
kVp	120	80,100,120,140,140/80,140/100
mA	35	100, 200, 300, AEC
D-FOV (mm)		400
S-FOV		L
Slice thickness (mm)		1
Reconstruction Kernel		Q40f medium
Pitch		0.6

Image evaluation

The CT images that clearly displayed the trachea were selected for evaluation. Using ImageJ image-processing software (ImageJ bundled with 64-bit Java 1.8.0.112, National Institutes of Health, Bethesda, MD, USA), a 25 mm² region of interest (ROI) was placed in the center of the ascending aorta, over which the signal intensity and standard deviation were measured. Additionally, an equivalent ROI was applied to an area 3 cm from the outer-central section of the ART phantom, which was used to measure the

background signal intensity and standard deviation. These values were substituted into Equation 1 to obtain the signal-to-noise ratio (SNR) and contrast-to-noise ratio (CNR) (equation 2) (figure 2) (6-7).

$$SNR = \frac{Background ROI SI - ROI SI}{ROI SD} \tag{1}$$

$$CNR = \frac{Background ROI SI - ROI SI}{\sqrt{Background ROI SD^2 + ROI SD^2}} \tag{2}$$

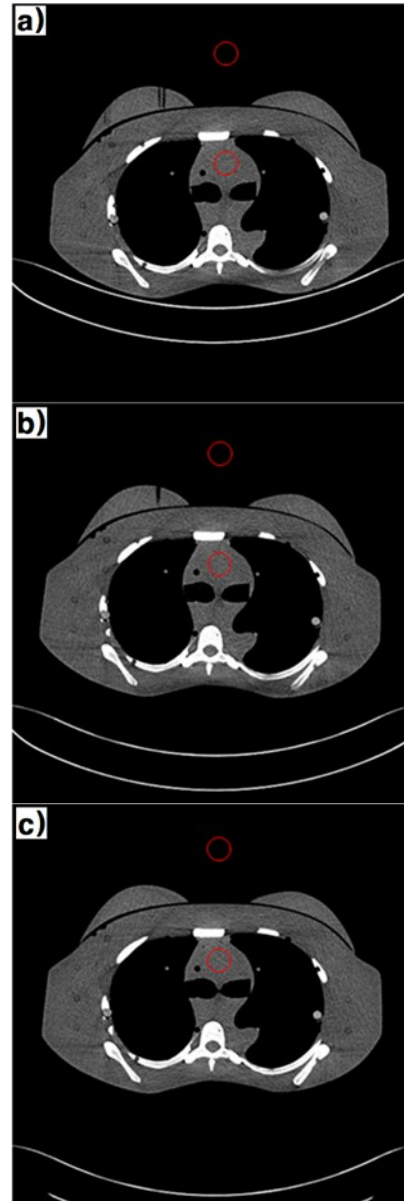


Figure 2. ART Phantom CT image Evaluation using SNR and CNR. a) 0 cm Air mattress, b) 5 cm Air mattress, c) 10 cm Air mattress.

Statistical analysis

Using SPSS Ver. 23.0 statistical analysis software package (IBM Corp., Chicago, IL, USA), the statistical significance was acquired using a paired *t-test* on the resultant changes in ESD and image quality for the three cases considered here, based on changes in the X-ray tube voltage and current. The confidence

interval was set to 95%, with p-values <0.05 considered as statistically significant.

RESULTS

Changes in ESD due to variations in X-ray tube voltage and current

Changes in the ESD due to changes to the X-ray tube voltage and current with and without an air mattress were measured, as displayed in table 2. When an air mattress was employed, a statistically significant reduction in ESD ($p < 0.05$) was observed for all X-ray tube voltages and currents.

Table 2. ESD measurements for different X-ray tube voltages and currents.

		Air mattress	N	Mean ± SD	p
kVp	80	None	60	4.77 ± 1.76	0.000*
		5cm	60	4.01 ± 1.52	
		10cm	60	4.18 ± 1.54	
	100	None	60	8.56 ± 3.55	0.000*
		5cm	60	7.56 ± 3.17	
		10cm	60	7.84 ± 3.32	
	120	None	60	13.55 ± 6.88	0.000*
		5cm	60	12.56 ± 6.14	
		10cm	60	12.81 ± 6.71	
	140	None	60	18.33 ± 9.02	0.000*
		5cm	60	16.70 ± 7.72	
		10cm	60	16.44 ± 7.32	
140/80	None	60	6.48 ± 2.20	0.000*	
	5cm	60	5.90 ± 2.24		
	10cm	60	5.97 ± 2.24		
140/100	None	60	10.87 ± 6.33	0.000*	
	5cm	60	10.21 ± 5.88		
	10cm	60	10.12 ± 5.73		
mA	100	None	90	6.01 ± 2.45	0.000*
		5cm	90	5.58 ± 2.43	
		10cm	90	5.68 ± 2.45	
	200	None	90	12.20 ± 5.28	0.000*
		5cm	90	11.06 ± 4.79	
		10cm	90	11.01 ± 4.69	
	300	None	90	17.66 ± 8.55	0.000*
		5cm	90	15.90 ± 7.80	
		10cm	90	16.10 ± 7.58	
	AEC	None	90	5.85 ± 2.36	0.000*
		5cm	90	5.42 ± 2.47	
		10cm	90	5.45 ± 2.38	

Unit: mGy. Index: paired t-test, * $p < 0.05$

Changes in SNR and CNR due to X-ray tube voltage variations

Changes in the SNR and CNR based on X-ray tube voltage variations with and without an air mattress

were measured, as displayed in table 3. When an air mattress was employed, a statistically significant increase in SNR and CNR ($p < 0.05$) was observed for all X-ray tube voltages.

Changes in SNR and CNR due to X-ray tube current variations

Changes in the SNR and CNR based on X-ray tube current variations with and without an air mattress were measured, as displayed in table 4. When an air mattress was employed, a statistically significant increase in SNR and CNR ($p < 0.05$) was observed for all X-ray tube currents.

Table 3. Calculated SNR and CNR values for different X-ray tube voltages.

		kVp	Air mattress	N	Mean ± SD	p
SNR	80		None	60	35.40 ± 7.46	0.000*
			5cm	60	36.30 ± 7.38	
			10cm	60	36.61 ± 8.46	
	100		None	60	53.34 ± 11.42	0.000*
			5cm	60	55.94 ± 11.99	
			10cm	60	54.16 ± 10.88	
	120		None	60	66.69 ± 14.94	0.000*
			5cm	60	68.30 ± 14.49	
			10cm	60	68.55 ± 13.88	
	140		None	60	76.39 ± 14.79	0.000*
			5cm	60	83.56 ± 17.63	
			10cm	60	80.80 ± 13.98	
	140/80		None	60	44.65 ± 8.90	0.000*
			5cm	60	45.94 ± 9.59	
			10cm	60	46.46 ± 9.60	
	140/100		None	60	60.61 ± 15.83	0.000*
			5cm	60	63.91 ± 16.42	
			10cm	60	62.86 ± 16.70	
CNR	80		None	60	31.54 ± 6.46	0.000*
			5cm	60	32.37 ± 6.21	
			10cm	60	32.65 ± 7.10	
	100		None	60	45.56 ± 8.51	0.000*
			5cm	60	46.89 ± 8.52	
			10cm	60	46.26 ± 8.00	
	120		None	60	54.49 ± 9.61	0.044*
			5cm	60	55.02 ± 9.61	
			10cm	60	55.53 ± 9.56	
	140		None	60	63.78 ± 11.88	0.000*
			5cm	60	65.48 ± 11.97	
			10cm	60	65.86 ± 11.16	
	140/80		None	60	35.40 ± 6.33	0.000*
			5cm	60	36.38 ± 6.89	
			10cm	60	36.99 ± 7.23	
	140/100		None	60	46.97 ± 10.56	0.000*
			5cm	60	48.81 ± 10.53	
			10cm	60	47.77 ± 10.19	

Index:paired t-test, * $p < 0.05$

Table 4. Calculated SNR and CNR values for different X-ray Tube currents.

	mA	Air mattress	N	Mean \pm SD	p
SNR	100	None	90	45.70 \pm 11.99	0.000*
		5cm	90	47.62 \pm 13.46	
		10cm	90	47.78 \pm 13.11	
	200	None	90	61.44 \pm 15.60	0.000*
		5cm	90	64.61 \pm 17.36	
		10cm	90	63.19 \pm 17.04	
	300	None	90	73.10 \pm 17.68	0.000*
		5cm	90	77.06 \pm 20.28	
		10cm	90	75.57 \pm 17.16	
	AEC	None	90	44.47 \pm 10.83	0.000*
		5cm	90	46.68 \pm 11.24	
		10cm	90	46.42 \pm 11.90	
CNR	100	None	90	38.64 \pm 10.01	0.000*
		5cm	90	39.51 \pm 9.91	
		10cm	90	39.95 \pm 10.15	
	200	None	90	50.33 \pm 12.36	0.000*
		5cm	90	52.03 \pm 13.23	
		10cm	90	51.35 \pm 13.01	
	300	None	90	58.44 \pm 13.45	0.000*
		5cm	90	59.54 \pm 13.15	
		10cm	90	59.86 \pm 12.48	
	AEC	None	90	37.74 \pm 8.77	0.000*
		5cm	90	38.88 \pm 8.77	
		10cm	90	38.88 \pm 9.35	

Index: paired t-test, *p<0.05

DISCUSSION

The purpose of the tables commonly used for diagnostic medical equipment that apply radiation is to move the patient at a constant speed without generating any distortion in the diagnostic images. However, if the table becomes exposed to radiation, the X-rays will scatter to various degrees, depending on the material of the table, which leads to an increase in the patient's ESD⁽⁴⁾.

Kang *et al.* covered the front and the rear areas of the patients to reduce the ESD caused by the scattered X-rays. The ESD measured higher in the rear area than in the frontal area; the authors determined that its cause was the scattered X-ray by the CT table⁽⁸⁾. This scattered X-ray increases the possibility of causing a radiation skin injury; moreover, it has been reported that necrosis and diseases that are caused by radiation, e.g., dermatitis, are extremely hard to cure^(3, 9-10).

A considerable amount of research has been carried out on reducing the patients' ESD due to scattered X-ray⁽¹⁴⁻¹³⁾. A previous study reported that the scatter radiation from the table could be reduced by increasing the distance between the table and the skin⁽¹⁴⁾. Another similar study reported that the same method could be applied to decrease the scattered X-ray that occurs from the radiation-shielding material⁽¹⁵⁻¹⁷⁾.

The research results showed that the ESD reduction effect by applying an air mattress was the

most effective at low X-ray tube voltages and high X-ray tube currents. And according to Bushong's study, the air-gap technique was found to be most effective for voltages less than 90 kVp⁽¹⁸⁾. From these results, it is considered that an air mattress would be highly useful in the CT screening of children, as it uses low X-ray tube voltages⁽¹⁹⁾.

In addition, while it was expected that the ESD reduction would be proportional to the air mattress thickness, the actual result showed that the ESD reduction and image quality improvement were greater for the 5 cm thick air mattress than the 10 cm thick air mattress. In a previous study⁽²⁰⁾, a foam pad was inserted between the radiation shielding material and the Phantom. The ESD and image quality were improved with a 1 cm thick foam pad; however, thicker foam pads provided no greater improvements.

The limitation of this study is that the image quality was only evaluated using the SNR and CNR; hence, further research is required before any future clinical application. Nevertheless, since it is extremely easy to reduce the ESD by applying an air mattress to the table of existing diagnostic medical equipment, and any kind of medical institution can immediately apply this method, it is expected that it can be effectively used to decrease patients' radiation doses.

CONCLUSION

An air mattress was manufactured to effectively reduce the scattered X-ray generated by a computed tomography table. After measuring the changes in the image quality and ESD, depending on the different X-ray tube voltages and currents, it was found that the application of a 5 cm thick air mattress provided a better image quality and excellent ESD reduction effect than cases without an air mattress or with a thicker mattress.

ACKNOWLEDGEMENTS

None.

Disclosure statement: No potential conflict of interest was reported by the authors.

Funding: None.

Ethical consideration: The authors declare no conflict of interest

Author contributions: All authors designed and wrote manuscript for this study.

REFERENCES

1. ICRP Publication 73 Ann. ICRP 26 (2) (1996) Radiological Protection and Safety in Medicine.
2. Kodyan J and Amber KT (2015) Topical antioxidants in radiodermatitis: a clinical review. *International Journal of Palliative Nursing*, 21 (9): 446-52.
3. Shim DM, Kim YM, Oh SK, Lim CM, Kown BT (2014) Radiation induced hand necrosis of an orthopaedic surgeon who had treated a

- patient with fluoroscopy-guided spine injection. *Journal of the Korean Orthopaedic Association*, **49**(3): 250-4.
4. Hong DH, Jung HR, Lim CH, Choi JG, Kim GJ (2015) A Study on the Compression Paddle Materials to Reduce Exposure during Mammography. *Indian Journal of Science and Technology*, **8**(26): 1-5.
 5. Meara SJ and Langmack KA (1998) An investigation into the use of carbon fibre for megavoltage radiotherapy applications. *Physics in Medicine & Biology*, **43**(5): 1359-66.
 6. Qi W, Li J, Du X (2009) Method for automatic tube current selection for obtaining a consistent image quality and dose optimization in a cardiac multidetector CT. *Korean Journal of Radiology*, **10**(6): 568-74.
 7. Lee WJ, Ahn BS, Park YS (2012) Radiation dose and image quality of low-dose protocol in chest CT: Comparison of standard-dose protocol. *Journal of Radiation Protection and Research*, **37**(2): 84-9.
 8. Kang YM, Cho JH, Kim SC (2015) Changes in entrance surface dose in relation to the location of shielding material in chest computed tomography. *Radiation Effects and Defects in Solids*, **170**(7-8): 645-50.
 9. Kodyan J and Amber KT (2015) Topical antioxidants in radiodermatitis: a clinical review. *International Journal of Palliative Nursing*, **21**(9): 446-52.
 10. Hoppe BS, Laser B, Kowalski AV, Fontenla SC, Pena-Greenberg E, Yorke ED, Lovelock DM, Hunt MA, Rosenzweig KE (2008) Acute skin toxicity following stereotactic body radiation therapy for stage I non-small-cell lung cancer: who's at risk?. *International Journal of Radiation Oncology Biology Physics*, **72**(5): 1283-6.
 11. Berg M, Bangsgaard JP, Vogelius IS (2009) Absorption measurements on a new cone beam CT and IMRT compatible tabletop for use in external radiotherapy. *Physics in Medicine & Biology*, **54**(14): 319-28.
 12. Court L, Urribarri J, Makrigrigios M (2010) Carbon fiber couches and skin sparing. *Journal of Applied Clinical Medical Physics*, **11**(2): 220-1.
 13. Seppälä JK, Kulmala JA (2011) Increased beam attenuation and surface dose by different couch inserts of treatment tables used in megavoltage radiotherapy. *Journal of Applied Clinical Medical Physics*, **12**(4): 15-23.
 14. Gray A, Oliver LD, Johnston PN (2009) The accuracy of the pencil beam convolution and anisotropic analytical algorithms in predicting the dose effects due to attenuation from immobilization devices and large air gaps. *Medical Physics*, **36**: 3181-91.
 15. Lee WH and Ahn SM (2014) Evaluation of reductive effect of exposure dose by using air gap apron in nuclear medicine related work environment. *The Journal of the Korea Contents Association*, **14**(12): 845-53.
 16. Jang DG, Kim CS, Kim JH (2015) Simulation of Energy Absorption Distribution using of Lead Shielding in the PET/CT. *J Korean Soc Radiol*, **9**(7): 459-65.
 17. Matyagin YV and Collins PJ (2016) Effectiveness of abdominal shields in chest radiography: a Monte Carlo evaluation. *The British Journal of Radiology*, **89**(1066): 20160465.
 18. Bushong S (2016) *Radiologic Science for Technologists: Physics, Biology, and Protection*. Elsevier Health Sciences.
 19. National Research Council (2006) *Health risks from exposure to low levels of ionizing radiation: BEIR VII phase 2*. National Academies Press.
 20. Kalra MK, Dang P, Singh S, Saini S, Shepard JO (2009) In-plane shielding for CT: effect of off-centering, automatic exposure control and shield-to-surface distance. *Korean Journal of Radiology*, **10**(2): 156-63.

